

Quasielastic-light-scattering study of the movement of particles in gels: Topological structure of pores in gels

Yoshiharu Suzuki and Izumi Nishio

Department of Physics, College of Science and Engineering, Aoyama Gakuin University, Tokyo 157 Japan

(Received 21 May 1991; revised manuscript received 16 September 1991)

A quasielastic-light-scattering study of polystyrene latex particles embedded inside a random system (in this case, polyacrylamide solutions and gels) was carried out. By measuring the correlation functions of the scattered-light intensity from suspended probe particles, structures of pores in gels were characterized. In the vicinity of the gelation threshold, the movement of particles in the gel may be quite different from normal diffusion, because of the interference from polymer networks. In this report the relation between the diffusion process and the correlation length of the system is discussed. The characteristic exponent of the topological structure of pores in gels at the threshold is also estimated.

Recently, many extensive studies of the structures of gels have been reported, using several experimental techniques such as light scattering,¹ small-angle x-ray² and neutron scattering,^{3,4} electron microscopy,⁵ etc. These investigations gave us very important information about gels. Investigations on the microscopic molecular structure of cross-linked molecules and polymer networks in gels have made remarkable progress. Still, studies on the mesoscopic structure of gels, e.g., topological structure of "connected pores" in gels, have made little progress. Here, the "connected pores" represent openings in gels, like an opening in Swiss cheese, which are surrounded by polymers and polymer networks composing the gel. In this paper we studied the mesoscopic structure of gels and its contribution to physical phenomena in gels. Note that our studies are not about the structure of polymer networks themselves, but about the structure of the connected pores. Studies of the structure of pores are important for the understanding of gels themselves, transport phenomena in gels, percolation problems,^{6,7} and so on.

Previously, we have published an experimental technique⁸ to investigate the topological structure of the pores, which are partitioned by polymer networks. Here we give a brief discussion. Our method is to embed monodispersed particles in gel samples and to analyze the movement of probe particles that pass through the connected pores of gels. This movement of particles in gels must depend strongly on the structures of connected pores of gels. Especially at the gelation threshold, a peculiar diffusion will be expected because of the structure of connected pores restricted by polymer networks. By measuring how the particles diffuse in gels, we can indirectly obtain information on the structures of connected pores in gels. In order to detect such microscopic motions of particles, we used the standard laser-light-scattering method.⁹ Such techniques are widely used to study the properties of congested solutions and gels and several kinds of probes such as polymer chains,^{10,11} polystyrene latex particles,¹²⁻¹⁵ and so on, are mainly used.

In a previous paper, we reported that the autocorrelation functions of the scattered-light intensity from the

trapped particles in the gel depend on the scattering vector \mathbf{k}_s , where k_s is $|\mathbf{k}_s|$. To discuss the movement of particles in the connected pores, which have characteristic length L , we define parameter S and efficiency E , which correspond to the ratio of the nondecaying part of the correlation function to the decaying part:

$$S = k_s L, \quad (1)$$

$$E = \frac{C(0) - C(\infty)}{C(\infty)}. \quad (2)$$

Here $C(\tau)$ is the autocorrelation function of the scattered-light intensity from particles at delayed time τ . The efficiency E is closely related to the parameter S : When S is much larger than unity— L is infinite (the particle is not trapped) or L is much larger than $1/k_s$ (the particle is trapped)—the efficiency E will be 1 because the observed motion of the particle is that of virtually free movement and $C(\infty)$ converges to 1. Therefore, from the value of the efficiency observed at $S \gg 1$, we cannot determine the real situation of a particle in the sample. Only if the efficiency E approaches 0 as k_s goes to zero can we verify that the particle is really trapped in the polymer network. The change of efficiencies with $1/k_s$, which were measured from suspended particles in the sample just above threshold, are shown in Fig. 1(a). It is believed that in this system some compartments of the polymer network exist, and the size of a compartment—which is characterized by L —is very large. At relatively small $1/k_s$ ($S \gg 1$), the efficiencies are nearly 1, and this result indicates that the particles diffuse freely at this length scale. But the larger $1/k_s$ is ($S \rightarrow 0$), the more the efficiencies approach zero. This tendency of the efficiency shows that the particles in the sample are captured by the gel network and the movement of particles is restricted inside of compartment. The k_s dependence of the efficiency with the pre-gel sample (polymer solution) is shown in Fig. 1(b). These efficiencies do not depend on $1/k_s$ and are almost 1 for any $1/k_s$. This result shows that the particles in this sample really are not trapped. Because L is regarded as

infinity in this sample, S becomes always larger than unity at any $1/k_s$.

From these conclusions, we adopted the efficiency E and S at $k_s \rightarrow 0$ as a good indicator to judge whether the particles within the system are trapped and to estimate the gelation point.

Now we discuss how the particles diffuse in the system at the gelation threshold. It is believed that, at threshold, the system behaves neither as a branched-polymer solution nor as a perfect gel on any scale of time and length, and that the correlation length of the system is infinite.

It is reasonable to assume that only one infinitely connected pore exists in such a system and that the particles in the connected pores can move all over this system. Therefore, because of a strong obstacle from the infinite network (branched polymer), particles transfer awkwardly around the connected pores (see Fig. 2). As schematically shown in Fig. 2, when a particle that was at point A at time 0 diffused to point B , the particle must make a detour along the trace shown by the dashed line, avoiding shaded portions where the particle cannot pass through. By investigating such complicated particle diffusion we

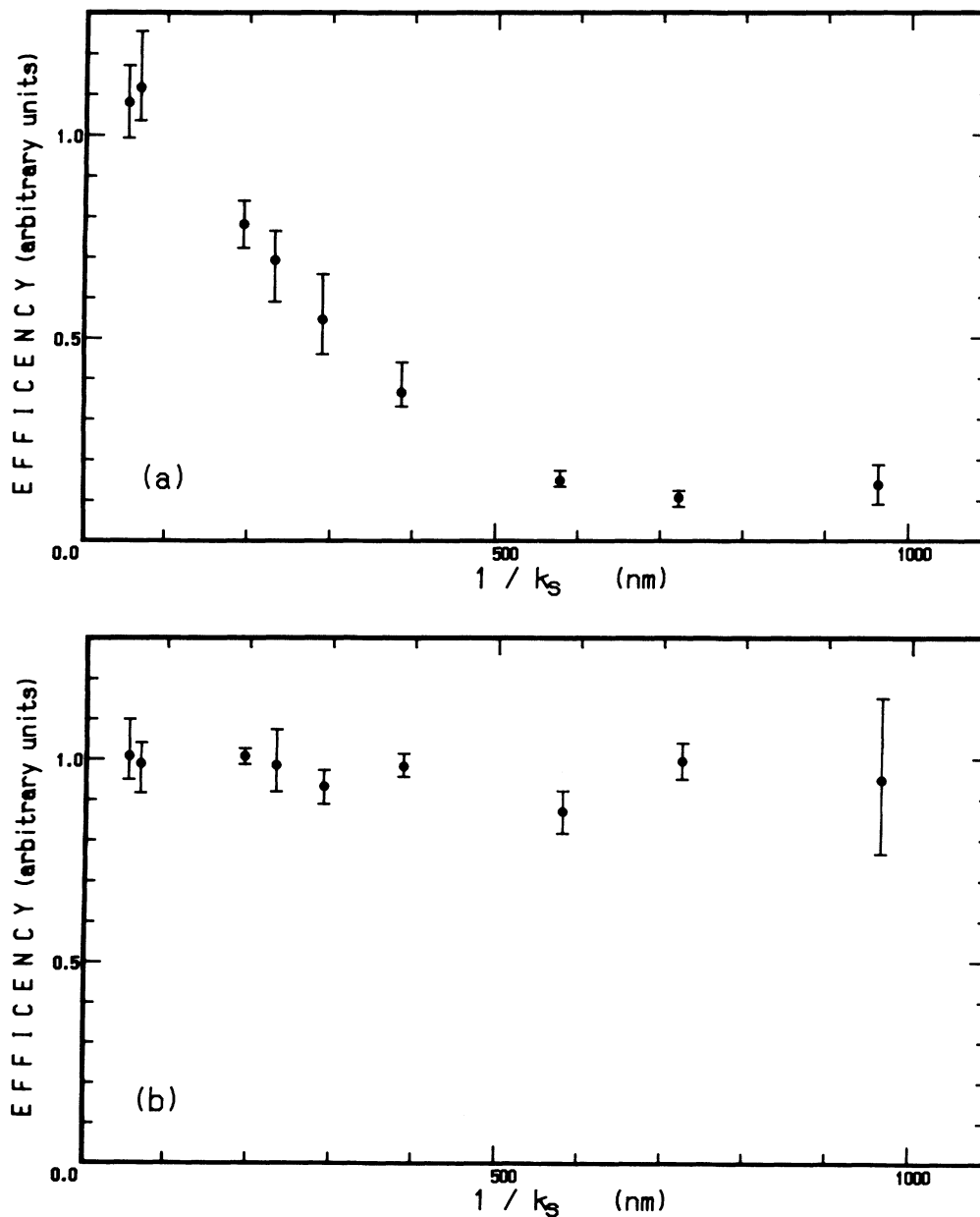


FIG. 1. $1/k_s$ dependence of efficiency, which is the ratio of the dc part of the correlation function to the decaying part of the correlation function. The efficiencies that were measured from samples above the gelation threshold are shown in (a). For efficiencies at small $1/k_s$, we cannot distinguish whether or not the particles are trapped by polymer networks. As $1/k_s$ increases, the efficiencies approach zero, indicating that particles are trapped by polymer networks. (b) describes efficiencies measured from the pre-gel sample (solution). Efficiencies are 1 at any $1/k_s$, and it is indicated that the particles in this sample are not trapped.

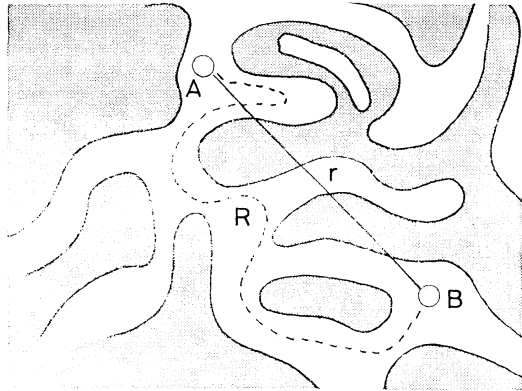


FIG. 2. Structure of pores in systems near the gelation threshold and the abnormal diffusion of the particle inside this sample shown schematically. The shaded portions correspond to dense polymer networks, which the particle cannot pass through. The particle must diffuse avoiding these polymer networks; for example, a particle at point *A* must move to *B* along the dashed curve. *R* is the distance that the particle actually moves and *r* is straight distance from *A* to *B*. Such a complicated structure of gels is reflected in the winding passage of the particle.

expect to obtain indirectly the characteristic information of the topological structure of connected pores in gels at the threshold. If this structure takes the self-similar structure as predicted at threshold, the relation between *R*, the distance which the particle actually moved, and *r*, the straight distance from point *A* to point *B*, should follow a power law as

$$R \sim r^\alpha, \quad (3)$$

where the power α represents the characteristic of the topological structure of connected pores at the gelation threshold. We assume that the time τ required for a particle to move from *A* to *B* is proportional to the square of *R* just as in normal diffusion. Thus the relation between τ and *r* is

$$\tau \sim R^2 \sim (r^\alpha)^2. \quad (4)$$

From (4) the square of *r* is

$$r^2 \sim \tau^{1/\alpha}. \quad (5)$$

The correlation function of the scattered-light intensity at the delay time τ is given by the Fourier transform of the probability distribution of the particle at time τ that was at the origin at time 0. If this probability distribution is similar to a Gaussian distribution, the autocorrelation function of the scattered-light intensity from a particle that diffuses in gel at gelatin threshold will be written as

$$C(\tau) = \exp(-Qk_s^2\tau^{1/\alpha}), \quad (6)$$

where the factor *Q* is a constant that depends on the diffusion coefficient

By taking the logarithm of $C(\tau)$, changing the sign, and taking logarithm again, the correlation function is reduced to

$$\begin{aligned} \log_{10}\{-\log_{10}[C(\tau)]\} \\ = \log_{10}[\log_{10}(e)] + 2\log_{10}(k_s) + \log_{10}(Q) + \frac{1}{\alpha}\log_{10}(\tau). \end{aligned} \quad (7)$$

By plotting $\log_{10}\{-\log_{10}[C(\tau)]\}$ against $\log_{10}(\tau)$, it becomes easy to analyze the movement and the behavior of particles in gel. If our argument holds, the plotted correlation function will form a straight line, and from slope of the correlation function we can deduce the value of the exponent α , which characterizes the structure of the gel. It is expected that if particles can freely diffuse in the system without obstacles such as branched polymers, this correlation function forms a straight line and the slope is 1. If the slope turns out to be smaller than 1, the correlation function may suggest some possibility of a peculiar diffusion process, which is different from normal diffusion.

To test the argument presented above, we have carried out experiments as follows. The samples used in these experiments are polyacrylamide gels and the solution made by copolymerizing acrylamide (AA) and cross-linking agent bis-acrylamide (bis), using ammonium persulfate as an initiator (40 mg/100 ml). Instead of using a catalyst, samples are formed by keeping the mixture at 80°C for 1 h.

A series of samples with the fixed cross-linking content $F_{\text{bis}}(=[\text{bis}]/([\text{bis}]+[\text{AA}])100)=1.1\%$, but with different total monomer concentration $F_{\text{tot}}(=[\text{AA}]+[\text{bis}])$ ranging from 0.5 to 2.5 wt.%, were prepared using the method described above. Before polymerization a small amount of polystyrene latex spheres (Latex), 1200 Å in diameter (from Sekisui, N-100) suspended in water was added to each pre-gel mixture. To prevent dust from entering into the samples, these samples are prepared in the clean area (class-10 environment by Hitachi), and the distilled water and mixture are passed through a membrane filter (0.22 μm from Millipore).

Because the scattered-light intensity from particles is about 100 times as strong as that from polymers, the scattered-light intensity observed in this experiment is virtually that of particles.

In this experiment the correlation functions do not have a single-exponential form but take multiexponential form. And each part of the correlation functions, which are sampled at a different clock time, has a unique relaxation feature. In order to observe every relaxation feature, we spliced several portions of the correlation functions, which are sampled at a variety of clock times. Figure 3 shows how we spliced functions *A* and *B*. For example, function *A* is sampled at a clock time of 1 sec and function *B* is sampled at 2 sec. Therefore the *n*th channel in function *B* and the 2*n*th channel in function *A* have the same delay time. We scale the fifth channel in function *B* with the tenth channel in function *A*, and normalize another channel in function *B* with the same scale.

Measurement of the correlation function of the scattered-light intensity from probes was performed using the standard quasielastic-light-scattering method. A laser-light-scattering apparatus is constructed around

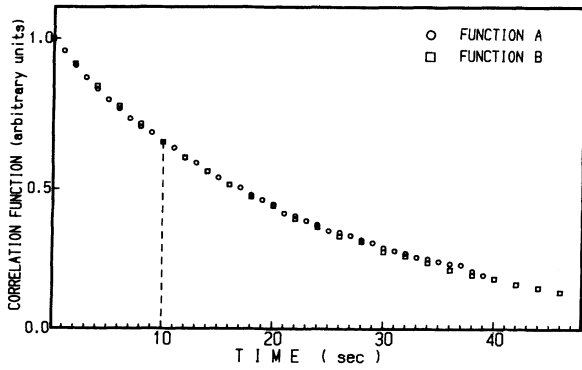


FIG. 3. Method of connecting the correlation functions, which were sampled at several clock times. Function *A* is shown, which was sampled at clock time 1 sec, marked by circles. Function *B*, which was sampled at 2 sec, is marked by triangles. The *n*th channel of function *A* and *n*th channel of function *B* have the same delayed time. In this case the fifth channel of function *B* is fitted with the tenth channel of function *A* and another channel of function *B* is normalized on the same scale.

35-mW helium neon-gas laser (wavelength 632.8 nm; NEC GLG5741) and a 64-channel multibit correlator (Kowa Z-216A). Control of the apparatus, the driving of goniometer, correlator, and so on, is done with a personal computer (NEC PC-9801 VM2).

All processes of measurement, except replacing samples, driving of this apparatus, analysis of the correlation function, recording of data, and so on, were carried out by computer. The correlation functions are also combined automatically by this computer.

Figure 4 shows the autocorrelation function of the scattered-light intensity from suspended particles in wa-

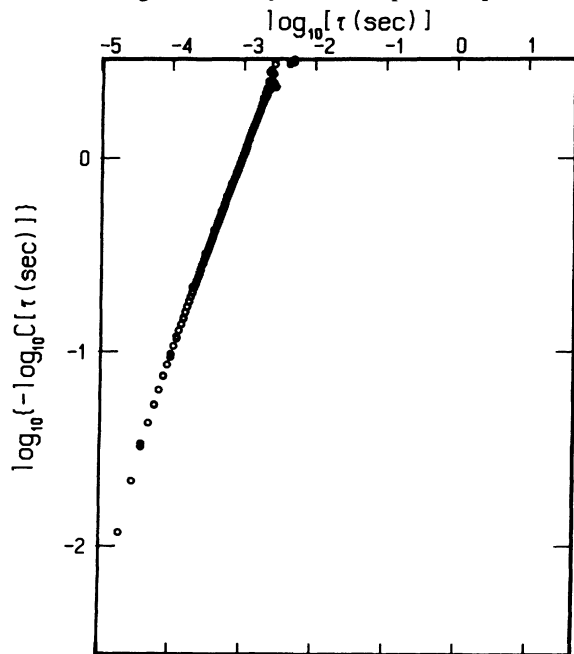


FIG. 4. Spliced correlation function of the scattered-light intensity from a 1200-Å polystyrene latex in water. Here this curve is not a solid line but is composed of a succession of data points.

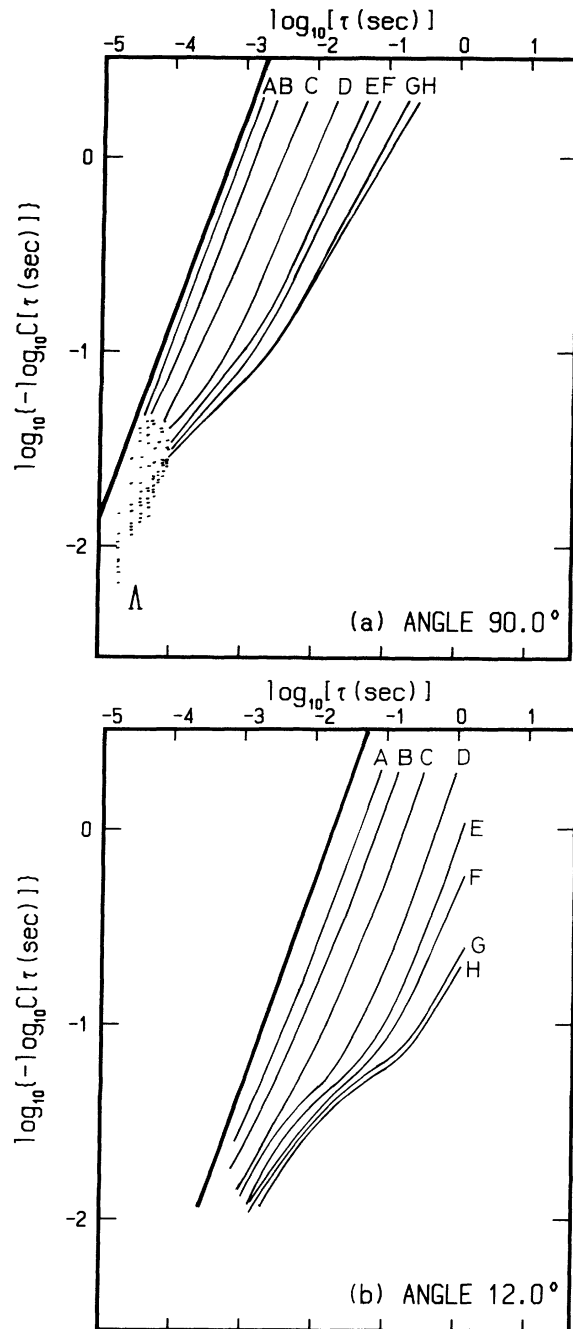


FIG. 5. Correlation functions of the scattered-light intensity from 1200-Å polystyrene latex embedded inside polyacrylamide samples with different total monomer concentration, F_{tot} (*A*, 0.50 wt. %; *B*, 1.00 wt. %; *C*, 1.50 wt. %; *D*, 2.00 wt. %; *E*, 2.20 wt. %; *F*, 2.30 wt. %; *G*, 2.40 wt. %; *H*, 2.44 wt. %), and with fixed cross-link content, $F_{bis} = 1.1\%$. The correlation function traced by the thick line is measured from the sample with cross-link content, $F_{bis} = 0\%$, and with $F_{tot} = 2.5\%$. These correlation functions are made from individual correlation functions measured with several different clock times. The spliced correlation functions $\log_{10}\{-\log_{10}[C(\tau)]\}$ are plotted against $\log_{10}(\tau)$ and the features after 100 μ sec are represented by solid lines for simplicity. However, correlation functions on part Λ in (a) are not simplified. Correlation functions shown in (a) were measured at a scattering angle of 90° ; correlation functions in (b) were at 12.01° .

ter. The size of the latex particles is 1200 Å in diameter. This curve is plotted using the foregoing method. The slope is unity and this result indicates that the particles in water diffuse normally.

Figure 5 shows the autocorrelation functions of the scattered-light intensity from suspended particles (1200 Å) in pre-gel samples, from F_{tot} of 0.50 to 2.44 wt. %. As the total monomer concentration increases, the extent of the branched polymers grows larger and the diffusion process of the particle in the sample becomes more complicated. All correlation functions shown in Fig. 5(a) were measured at a scattering angle of 90.00°. The thick line in this figure corresponds to the correlation function of the scattered-light intensity from particles in no cross-linked sample ($F_{\text{bis}}=0\%$), and the slope is exactly as expected for normal diffusion in a simple linear polymer solution. As F_{tot} increases, the correlation functions shift to the right, indicating the decrease in the diffusion coefficient of the probe or the increase in viscosity of the system. We can also see that the slope of the correlation function becomes smaller with F_{tot} . This fact indicates that the diffusion process of particles in the pre-gel sample differs from normal diffusion by the effect of growth of a branched-polymer structure as F_{tot} increases. At short delay time, before 100 μsec , the slope of correlation functions were close to 1. This part is identified by marker Λ . It is so illegible that the curves on this part were not identified. This result suggests the existence of a narrow space where a particle can diffuse freely and where the influence of polymers on the diffusion process seems negligible.

The correlation functions shown in Fig. 5(b) were measured at the scattering angle of 12.01° from a series of samples. These correlation functions, which were observed with longer spatial wavelength than those at 90°, contain information on the diffusion process for a long time scale and longer range. As shown in Fig. 5(b), the diffusion between 1 and 100 msec is similar to ones shown in Fig. 5(a). After about 100 msec, for lower F_{tot} , the slope of the correlation function becomes steeper and returns to unity, which indicates a change from abnormal diffusion to normal diffusion. But as the value of F_{tot} approaches the gelation point, the slope hardly returns to unity. It is assumed that this change of slope depends on the correlation length ξ , a characteristic size of the structure of space in these systems. In general, when the system is observed at a shorter range than ξ , it has a self-similar structure but, for longer range than ξ , the structure is no longer self-similar. It is believed that the correlation length of the system becomes longer with F_{tot} , and that at the exact threshold it diverges. For the case of finite correlation length, if the relative diffusing distance of the particles in this sample is shorter than the ξ of the system, the diffusion process of particles seems abnormal because of the influence of self-similar structure on the movement of particles. If the relative diffusing distance is greater than ξ , the diffusion process seems to be normal diffusion (random walk), whose step corresponds to the correlation length ξ , as schematically shown in Fig. 6. From such assumptions the change of slope as seen in Fig. 5(b) can be explained as the change from abnormal

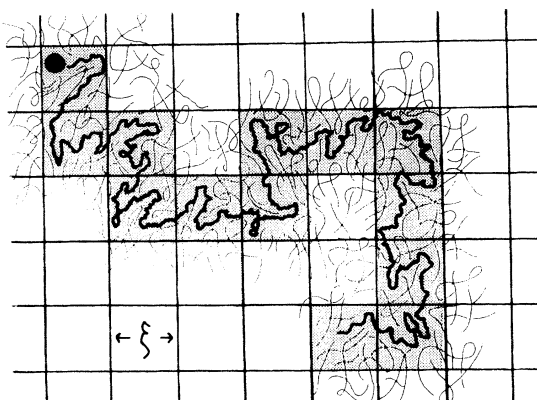


FIG. 6. Diffusion process of a particle in a branched-polymer solution with finite correlation length ξ . When the measurement is at a shorter range than the correlation length ξ , the recognizable behavior of the particle is shown by the thick line and is abnormal diffusion because of the obstacles, namely, polymer branches. But when the range is larger than ξ , the behavior is observed as a random walk whose step is ξ (a shaped portion is helpful at this point).

diffusion to normal diffusion. At the threshold it is expected that the slope of the correlation function persists because of the diverging correlation length of the system, which corresponds to the characteristic size of connected pores in the gel. Therefore, by measuring the slope of the correlation function at the threshold, the exponent α , which characterizes the topological structure of the pore in this system, can be estimated.

The correlation function shown in Fig. 7 is of

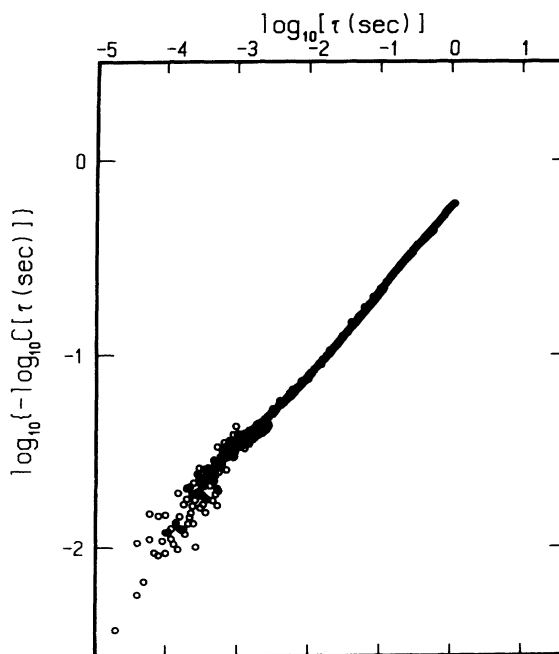


FIG. 7. In the vicinity of the gelation point, the correlation function of scattered-light intensity from probe particles in gels with $F_{\text{tot}}=2.48$ wt. % and with $F_{\text{bis}}=1.1\%$. This correlation function is composed of a succession of data points.

scattered-light intensity from particles in the sample, which is found to be closest to the gelation point, with $F_{\text{tot}} = 2.48$ wt. %. The gelation point was verified by macroscopic observation. The curve of the correlation function is almost a straight line and the slope is constant for all time scales observed. These facts conform to our foregoing idea. From the slope, α was estimated to be 2.1 ± 0.1 . The fractal dimension of the connected pore's structure in gels at threshold is a little larger than the fractal dimension of a random walk in free space. It is found that the relation between the time τ and relative distance r will be

$$\tau \sim r^{4.2} \quad (8)$$

The anomalous diffusion in complex media as measured in this experiment was discussed by Havlin and Ben-Avraham.¹⁶ They predicted that the exponent, which corresponds to the exponent in Eq. (8), was 4 in three dimensions. It is interesting to compare their prediction with our result; our exponent is 4.2, which is very close to theirs.

The correlation function shown in Fig. 8 was observed from the diffusion of particles in a sample where the polymer construction exceeded the gelation point. It is expected that in such a system polymer networks have been already constructed and that particles were trapped by the networks. Thus the correlation function will be different from the one shown in Fig. 7. In part *A* of Fig. 8, the slope of the correlation function is about unity, indicating free diffusion. (The slope of the solid line in part *A* is unity.) After a time delay of 100 μsec , the displacement follows a power law with an exponent of 2.1, and this value is the same as shown in Fig. 7. (The slope 2.1 is indicated by the solid line.) If the polymer concentration of this sample is the critical concentration needed for gelation, the slope of the curve should be constant. However, the slope in part *C* becomes more gentle than that of part *B*. This deviation from a power law is a direct re-

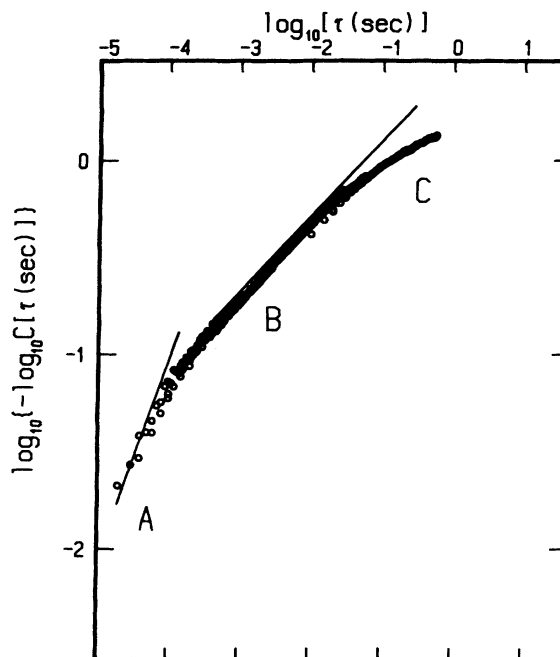


FIG. 8. Spliced correlation function of the scattered-light intensity from particles in a sample whose concentration exceeds slightly the critical concentration needed for gelation. Here this curve is not a solid line but is composed of a succession of data points. The slope of the guideline in part *A* is unity and the slope in part *B* is 2.1.

sult of gelation and the trapping of particles by the infinite-polymer network. It was observed that the ratio of part *C* to part *B* becomes large as cross-link content increases.

For the meaning of the value of the exponent α and of the diffusion in media above the gelation point, we have to await future studies and discussions.

¹T. Tanaka, D. J. Fillmore, S. T. Sun, I. Nishio, G. Swislow, and A. Shah, *Phys. Rev. Lett.* **38**, 1636 (1980).

²M. Djabourov, A. H. Clark, D. W. Rowlands, and S. B. Ross-Murphy, *Macromolecules* **22**, 180 (1989).

³T. P. Hsu and C. Cohen, *Polymer* **25**, 1419 (1984).

⁴S. Candau, J. Bastide, and M. Delsanti, *Adv. Polym. Sci.* **44**, 27 (1982).

⁵E. Bouchaud, M. Delsanti, M. Adam, M. Daoud, and D. Durand, *J. Phys. (Paris)* **47**, 1273 (1986).

⁶P. G. de Gennes, *Scaling Concepts in Polymer Physics* (Cornell University Press, Ithaca, NY, 1979).

⁷D. Stauffer, *Introduction to Percolation Theory* (Taylor & Francis, London, 1985).

⁸I. Nishio, J. C. Reina, and R. Bansil, *Phys. Rev. Lett.* **59**, 684

(1987).

⁹B. Chu, *Laser Light Scattering* (Academic, New York, 1974).

¹⁰R. H. Ottewill and N. St. J. Williams, *Nature* **325**, 232 (1987).

¹¹K. L. Yam, D. K. Anderson, and R. E. Buxbaum, *Science* **241**, 330 (1988).

¹²F. Madonia, P. L. San Biagio, M. U. Palma, G. Schiliro, S. Musumeci, and G. Russo, *Nature* **302**, 412 (1983).

¹³N. L. Gershfeld, W. F. Stevens, Jr., and R. J. Nossal, *Faraday Discuss. Chem. Soc.* **81**, 19 (1986).

¹⁴J. Newman, N. Mroczka, and K. L. Schick, *Biopolymers* **28**, 655 (1989).

¹⁵J. Newman, K. L. Schick, and K. S. Zaner, *Biopolymers* **28**, 1969 (1989).

¹⁶S. Havlin and D. Ben-Avraham, *Adv. Phys.* **36**, 695 (1987).

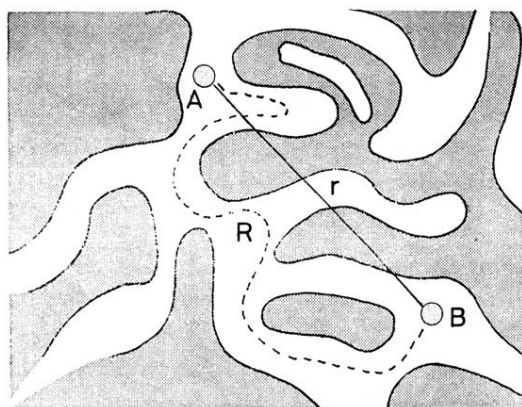


FIG. 2. Structure of pores in systems near the gelation threshold and the abnormal diffusion of the particle inside this sample shown schematically. The shaded portions correspond to dense polymer networks, which the particle cannot pass through. The particle must diffuse avoiding these polymer networks; for example, a particle at point *A* must move to *B* along the dashed curve. *R* is the distance that the particle actually moves and *r* is straight distance from *A* to *B*. Such a complicated structure of gels is reflected in the winding passage of the particle.

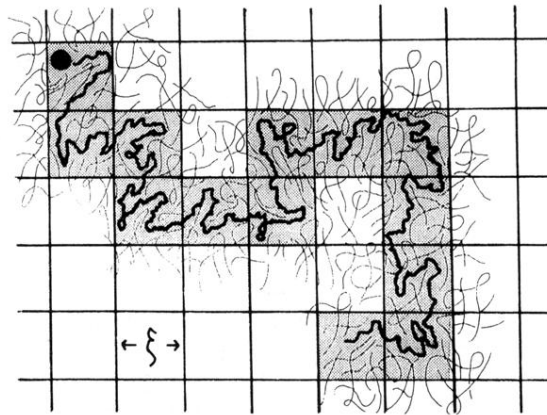


FIG. 6. Diffusion process of a particle in a branched-polymer solution with finite correlation length ξ . When the measurement is at a shorter range than the correlation length ξ , the recognizable behavior of the particle is shown by the thick line and is abnormal diffusion because of the obstacles, namely, polymer branches. But when the range is larger than ξ , the behavior is observed as a random walk whose step is ξ (a shaped portion is helpful at this point).